

Influence of Polyethylene and Carbon Black Morphology on Void Formation in Conductive Composite Materials: A SANS Study

J. Oakey and D. W. M. Marr*

Chemical Engineering Department, Colorado School of Mines, Golden, Colorado 80401

K. B. Schwartz and M. Wartenberg

Raychem Corporation, 300 Constitution Dr., Menlo Park, California 94025

Received February 5, 1999; Revised Manuscript Received May 27, 1999

ABSTRACT: The effects of carbon black filler and polyethylene matrix morphology on void formation in conductive composites have been studied by small-angle neutron scattering. Void formation was observed to occur postprocessing during polyethylene crystallization as a result of filler particle/polymer matrix interactions. Carbon black structure, concentration and polymer crystallinity were identified as critical parameters in this process that can be combined and used to predict void content in these semicrystalline composite materials.

Introduction

Conductive composites are commonly manufactured by blending a semicrystalline polymer with conductive filler such as carbon black above its percolation threshold. Under such conditions, the filler maintains a conductive pathway through the insulating polymer matrix until sufficient heat generated by resistance within the system melts crystalline domains and expands the semicrystalline polymer.¹ During melting, the density of the overall polymer phase is reduced, and as the percolation threshold is approached, the composite undergoes a transition from conductive to highly resistive.^{2–4} For constant-voltage situations, this greatly reduces the current, the polymer cools, and the composite returns to its original morphology and function. This phenomenon, known as the positive temperature coefficient (PTC) effect, can be manipulated for many applications including self-regulating heaters and resettable fuses.^{5,6}

While simple and inexpensive, the production of these composites is hindered by morphological variations resulting from changes in processing conditions. Since the reproducibility of the PTC effect is sensitive to morphology, there is strong motivation to understand how variations in composition and processing conditions influence microstructure in these composites. Previously, small-angle neutron and X-ray scattering (SANS and SAXS) have been used to investigate the carbon black particle size and spacing within a polyethylene matrix.⁷ The conductivity of the composite, which occurs as a result of tunneling between percolating particles giving rise to the PTC effect, is strongly affected by such particle morphology.⁷ Scattering data from these studies of similar carbon black/polyethylene composites suggested the presence of an additional phase. Dubbed the “void” phase, its existence complicates the composite morphology and may threaten the reproducibility of the sensitive PTC effect either via morphological variation within the composite or catastrophic failure. The hypothesis that this phase exists within the composites was reinforced by pycnometry, which revealed a con-

sistently lower experimental density than predicted. The authors suggested that voids were formed as a result of incomplete adhesion or wetting of the polyethylene to the carbon black particles.⁷

Subsequent studies have focused on the application of SANS as a technique to characterize the void phase within conductive composites. SANS has proven to be a valuable characterization technique in studying void content in conductive composites due to the small wavelength of neutrons (5–15 Å) and the ease with which contrast can be varied between the polymer and filler phases, thus accentuating the void phase. These studies have successfully demonstrated that size and quantity of voids can be determined using an analysis for three-phase composites originally described by Wu.^{8,9} The observation from these experiments that void content increases with carbon black volume fraction led to the hypothesis that filler surface area influences void development. Additionally, temperature excursions were performed with composites to study the behavior of the void phase at ambient conditions and in the melt. These experiments illustrated that voids virtually disappear in the melt, suggesting the mechanism for incorporation is closely related to postprocessing recrystallization of the polyethylene matrix.

This article describes our investigation into the mechanism by which voids form in conductive composites amid percolating networks of carbon black. To test our hypothesis that voids form upon recrystallization and the extent of their development is correlated with the amount of filler surface area, we employ SANS to probe the void phase of conductive composites formulated with carbon blacks of varying structure and volume fraction. To exploit the utility of SANS, we prepared duplicate composites with both deuterated and protonated polyethylene. Through comparison of SANS results generated by these two composites of different neutron contrast, the void volume fraction can be readily calculated. To verify the morphological similarity between composites prepared with protonated and deuterated polyethylene (hPE and dPE, respectively), SAXS can be employed because of its insensitivity to isotopic substitution.

* Corresponding author.

Table 1. Scattering Length Densities (SLD, 10¹⁰ cm⁻²)

species	density (g/cm ³)	amorphous SLD	crystalline SLD	total SLD
<i>h</i> -polyethylene (hPE)	0.953 ± 0.001	-0.3	-0.36	-0.34
<i>d</i> -polyethylene (dPE)	1.080 ± 0.002	7.3	8.58	8.13
carbon black (CB)	1.80 ± 0.002			6.4
voids				0

Theoretical Background

As reported in a previous paper,⁸ it is possible to use SANS to determine the size and volume fraction of voids in carbon black/polyethylene composites by employing a three-phase, invariant-based analysis originally discussed by Wu.⁹ In composites of hPE and carbon black nearly all coherent scattering arises as a result of the apparent two-phase morphology since the scattering length density (SLD) of both the polymer and the void phases is essentially zero (see Table 1). Because there is virtually no SANS contrast between the void and polyethylene phases, a two-phase model may be employed for convenient analysis. Figure 1 is a transmission electron micrograph (TEM) image of a carbon black/polyethylene composite, which suggests a random two-phase morphology model would be appropriate. Such a model is the Debye–Bueche model¹⁰

$$\frac{d\Sigma(q)}{d\Omega} = \frac{d\Sigma(0)}{d\Omega} (1 + q^2 a_c^2)^{-2}$$

where q represents the momentum transfer or scattering vector

$$q = \frac{4\pi}{\lambda} \sin(\theta/2)$$

λ is the neutron wavelength, θ the angle of scatter, and a_c the correlation length. Knowledge of a_c allows one to calculate domain sizes or chord lengths, l , of discrete phases.

This model works well for protonated systems in which the virtually identical SLD's of hPE and voids highlight the carbon black structure. To observe the structure of the void phase, dPE is substituted for hPE during preparation of the composite and a three-phase system is effectively created. Because of this substitution, fits of the single correlation length Debye–Bueche model to the SANS cross sections of these three-phase composites are generally poor. Therefore, for deuterated systems, we employ the two-correlation length Debye–Bueche model,^{11–13}

$$\frac{d\Sigma(q)}{d\Omega} = \frac{A_1}{1 + q^2 a_2^2} + A_2 \exp\left(-\frac{q^2 a_2^2}{4}\right)$$

where

$$\frac{d\Sigma(0)}{d\Omega} = A_1 + A_2$$

By now assuming that the void content is small and the morphologies of protonated and deuterated composites are identical, one can determine the volume fraction and chord length of the void phase by comparing the

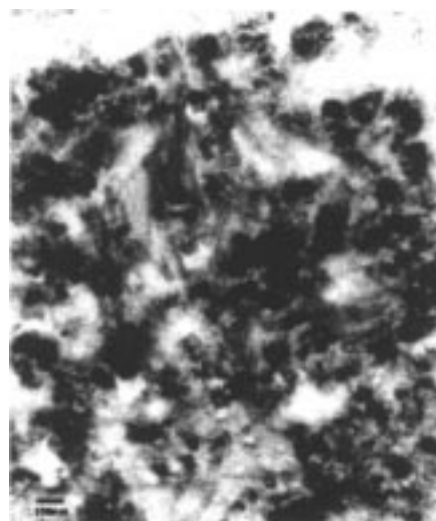


Figure 1. A TEM image of a carbon black/polyethylene composite demonstrates the random two-phase morphology of the system.

two- and three-phase composite scattering integrated intensities. Details of these calculations are given in ref 8.

The calculations of void content and size, however, are sensitive to composite composition. Therefore, we correct for temperature excursions in which the effective volume fractions of the polymer and filler phases are changing due to polyethylene melting and expansion. The new composition is predicted through the melt by

$$\phi_2^{\text{new}} = \frac{1}{1 + \frac{d_{\text{PE}}^{\text{t}}}{d_{\text{PE}}^{\text{a}}} \left(\frac{1}{\phi_2^{\text{old}}} - 1 \right)}$$

where d_{PE}^{a} is the density of the amorphous polymer phase and d_{PE}^{t} is the total density of the polymer phase at a given temperature.

To apply this invariant analysis and obtain accurate void content data, the microstructures of both the protonated and deuterated composites must be identical. To verify this assumption, we employed SAXS to investigate the nanostructure of each composite. As SAXS is insensitive to fluctuations in scattering length density, overlapping protonated and deuterated SAXS signals indicate identical composite morphology.⁸ To quantify the similarity of the SAXS data without resorting to a specific model to describe the complex morphology, we calculate an integrated intensity

$$\int_{q_{\text{min}}}^{q_{\text{max}}} q I(q) dq$$

where q_{min} and q_{max} represent the measurable range of the scattering vector over which the intensity is rigorously integrated from experimental data measured using a slit source.

Experimental Approach

Sample Preparation. Experiments were conducted with composites of carbon black volume fractions ranging from 0.085 to 0.429 using a lamp black of high structure and furnace blacks of medium and low structure (see Table 2). Each carbon black at a particular volume fraction was separately compounded into hPE and dPE. Composites were prepared in a DACA small-scale twin-screw minicompounder,¹⁴ a mixer/

Table 2. Carbon Black Characteristics

carbon black structure	primary particle size, ²² <i>a</i> (nm)	DBP number ²³ (mL/100 g of CB)
high	95	112
medium	82	80
low	56	46

extruder designed for formulations of 1–5 cm³. Carbon black was added to each polyethylene to achieve the appropriate volumetric composition at a constant total mass of 3 g and mixed at 190 °C and 100 rpm for 5 min in the DACA minicomponenter.

From the extruded composite material, 3 in. square slabs were pressed at 205 °C and 10 000 lb to a thickness of 0.014 in. using a hydraulic press. These slabs were then inserted into another press at the same pressure and brought to 25 °C with cooling water. The slabs were subsequently punched into 5/8 in. diameter disks and annealed by heating from room temperature to 170 °C at a rate of 2 °C/min. After being held for 90 min at 170 °C, quenched samples were removed and plunged into an ice-water bath while annealed samples were first brought to 100 °C at 0.5 °C/min and then to room temperature at 2 °C/min.

Pure dPE samples were also made by the same procedures as the quenched and annealed composites in order to determine the background void content of polyethylene. The single correlation length Debye–Bueche model was fit to the data and used to calculate an invariant which was then employed to compute the volume fraction of the void phase. Upon carrying out this procedure, we obtained a consistent value of 0.0006 for the void volume fraction. This relatively small value was weighted by the polyethylene volume fraction and subtracted from all subsequent composite void content calculations as background. The remaining void volume fraction is solely a result of interactions among the polymer and filler particles.

Small-Angle Neutron Scattering (SANS). Scattering experiments were performed on the 30 m SANS beamline (NG-7) at the National Institute of Standards and Technology Center for Neutron Research in Gaithersburg, MD. The incident neutron beam of wavelength 5 Å was collimated by source and sample slits separated by a distance of 7.5 m. The sample–detector distance was 17.5 m, which gave an effective *q* range of 0.0002 Å^{−1} < *q* < 0.048 64 Å^{−1}. The exceptions to this procedure were the three experiments performed with composites formulated at a carbon black volume fraction of 0.085. In these cases, the wavelength of the incident neutron beam was 6 Å, giving an effective *q* range of 0.0002 Å^{−1} < *q* < 0.035 23 Å^{−1}. Over the entire *q* range, all scattering data were corrected on a cell by cell basis for instrumental backgrounds and detector efficiency variation, divided by the sample transmission and thickness and normalized to a constant incident flux. The net intensities were converted to an absolute differential scattering cross sections [dΣ/dΩ(*q*)] per unit sample volume (in units of cm^{−1}) via precalibrated secondary standards.¹⁵ Incoherent scattering, due primarily to protons in hPE, was calculated and subtracted according to a procedure described previously.¹⁶

Small-Angle X-ray Scattering (SAXS). SAXS measurements were performed on a Kratky compact small-angle system equipped with a programmable step scanner and gas-filled proportional detector.^{17,18} Cu Kα radiation was generated by a 12 kW rotating anode operating at 40 kV and 40 mA and selected by a graphite monochromator (λ = 0.154 nm). The incident line-focused beam upon the sample measured 150 μm × 14 mm and was attenuated to a typical intensity of 2.1 × 10⁷ photons/s. The sample-to-detector distance was 20 cm. Data were collected by scanning over 2θ = 0.13°–8.8°, resulting in a *q* range from 0.09 to 6.212 nm^{−1}. The raw SAXS data, in terms of detector counts per second, were corrected for background radiation and normalized for the direct beam intensity and composite absorption coefficient, yielding an absolute intensity in units of cm^{−1}.

Wide-Angle X-ray Scattering (WAXS). WAXS data were collected in order to determine the crystallinity of the poly-

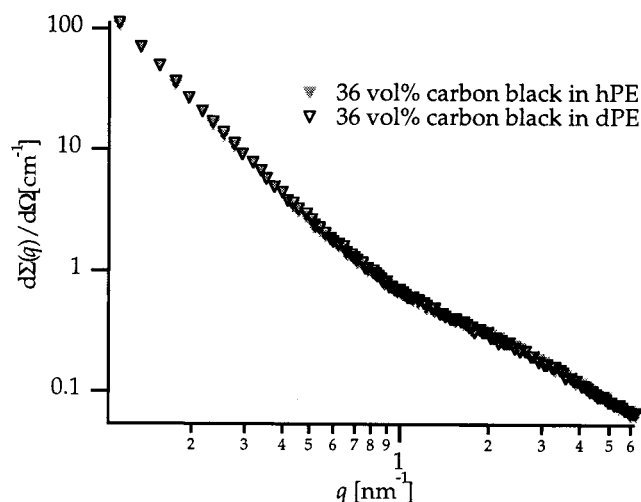


Figure 2. SAXS data from 36 vol % carbon black filler composites formulated with protonated and deuterated polyethylene. Overlapping absolute intensities indicate identical composite morphologies.

ethylene. The data were collected on a Siemens D500 powder diffractometer equipped with a single-crystal quartz incident-beam monochromator and a Braun one-dimensional position-sensitive detector. The samples rested on a glass holder. Data were collected at 5°/min and 0.02°/step in the range from 2θ = 10°–40° using Cu Kα₁ radiation (λ = 0.154 nm). Crystallinity was calculated from the integrated areas of the polyethylene diffraction peaks and amorphous halo which were determined by profile fitting of the X-ray diffraction pattern using a pseudo-Voigt function and a linear background correction.¹⁹ The amorphous scattering contribution of the carbon black is also accounted for during profile fitting.

Results and Discussion

Figure 2 displays representative SAXS signals for composites formulated with hPE and dPE. The overlapping scattering curves indicate identical composite morphology over the length scales investigated by our measurements. This qualitative observation can be quantified by calculation of the integrated intensity over the available range of *q*. Results of these calculations, which simply quantify the overall amount of scattered intensity from a given composite, are summarized in Table 3. Integrated intensities for hPE and dPE composites differ by only a small degree, indicating features within the respective composites are identical, including voids, and allowing the assumption of identical composite morphology required by our void analysis.

Figure 3 shows typical SANS cross sections for protonated and deuterated composites where the dPE scattering curves display a peak at high *q*, indicating a higher density crystalline phase. The dPE/carbon black composite scattering curve has been multiplied by the scattering invariant ratio

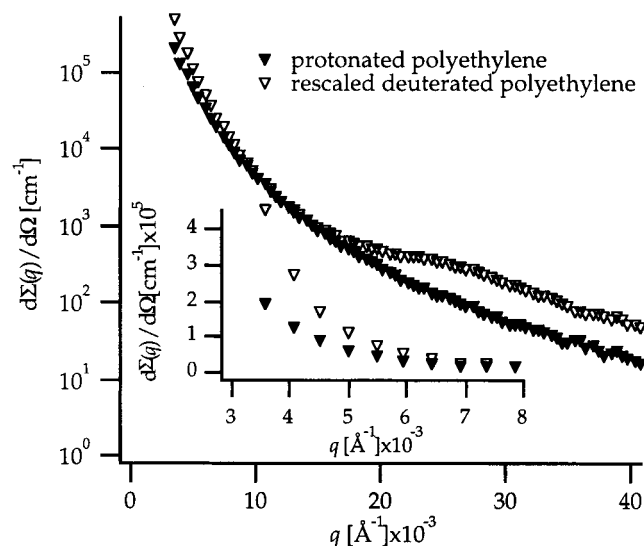
$$\frac{d\Sigma^\circ(q)/d\Omega}{d\Sigma(q)/d\Omega} = \frac{(\rho_{cb} - \rho_{hpe})^2}{(\rho_{cb} - \rho_{dpe})^2}$$

in order to overlap the hPE/carbon black composite scattering signal and illustrate deviations at low *q*. This low-*q* excess scattering indicates the presence of the void phase occurring in the dPE/carbon black composite.

As noticed in previous studies, the void phase virtually disappears in amorphous polyethylene/carbon black composites.⁸ This observation suggests that the forma-

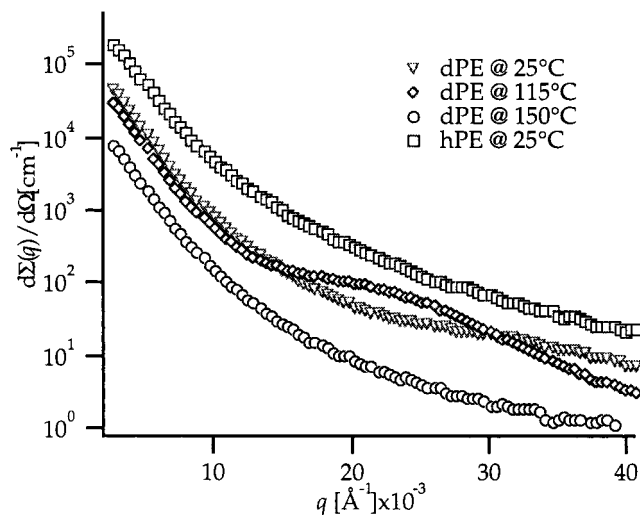
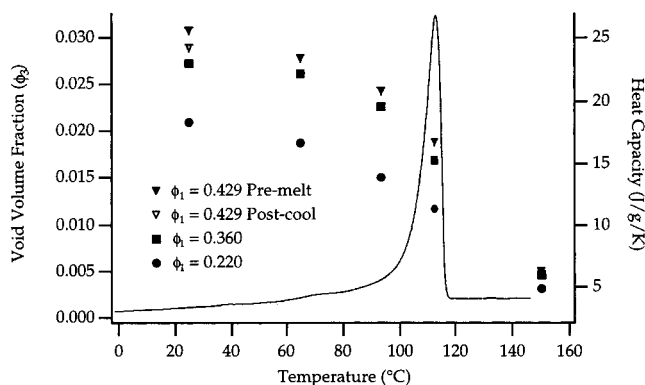
Table 3. Integrated SAXS Intensity Comparison (Annealed Samples, DBP = 80)

ϕ_1	hPE composite (cm ⁻³)	dPE composite (cm ⁻³)	% diff
0.22	176.15	194.75	9.55
0.29	225.53	236.5	4.64
0.36	271.52	276.32	1.74
0.429	276.32	294.26	6.10

**Figure 3.** SANS scattering from 42.9 vol % dPE/carbon black and hPE/carbon black samples at room temperature where the deviation at low q is due to scattering from voids. Error bars are omitted to clarify the chart data. The inset plot shows the low q data plotted on a linear-linear scale and clearly shows the significant excess void scattering.

tion of crystalline domains within the polymer phase leads to the incorporation of voids. To verify this, temperature excursions were performed in which samples were heated above the melt and then allowed to cool to room temperature while scattering data were collected. Figure 4 shows scattering data from a dPE/carbon black composite over a range of temperatures from the melt through ambient. In the melt the scattered intensity is significantly lower because of the lower SLD of amorphous relative to crystalline dPE. If the data are rescaled by the invariant ratio, one finds the amorphous dPE and semicrystalline hPE curves overlap at low values of measured q , as expected.

Figure 4 also demonstrates morphological variations in the crystalline domains during the cool as the crystalline peak shifts to higher q . As hypothesized, the formation of a crystalline phase appears to be linked to void development. Figure 5 displays the void content calculated via eq 1 of various composites vs temperature during the composite cool superimposed upon a pure dPE differential scanning calorimetry (DSC) cooling curve. Here, it can be seen that the void contents of the samples are essentially zero in the melt and increase steadily with the onset of dPE crystallization. At the end of this experiment, the composites have returned to room temperature as well as essentially the same void content measured before melting. These data indicate that void incorporation is clearly linked to the crystallization process of polyethylene and occurs in a reversible, nonstochastic manner. We have demonstrated that polyethylene crystallization induces relatively little void formation in pure polymer samples. We have also seen that purely amorphous polyethylene/carbon black com-

**Figure 4.** SANS scattering from 36 vol % carbon black samples at room temperature and through the melt.**Figure 5.** Void content from composites formulated with medium structure carbon black at various volume fractions as a function of temperature. Void content data are superimposed upon a DSC cooling curve, illustrating the correlation between the onset of crystallization and void formation.

posites are virtually free of voids while semicrystalline composites incorporate voids to a significant degree. Clearly, crystallization alone cannot explain void formation so interactions between the filler particles and the polyethylene matrix must play a significant role. To investigate the physical mechanisms through which voids form during polyethylene crystallization, we examine factors affecting the nature and extent of the polymer/filler interface, namely carbon black structure and volume fraction. To do so, carbon blacks of low, medium, and high structure were formulated into composites at five volume fractions ranging from 0.085 to 0.429. Figure 6 summarizes the results of these experiments for annealed samples and clearly demonstrates that void content increases with both increasing carbon black structure and volume fraction.

It is evident from data presented thus far that three primary factors affect the incorporation of voids within composites of carbon black and polyethylene: particle structure, filler concentration, and polyethylene crystallinity. Our results demonstrate the sensitivity of void formation to each of these factors individually; however, they also suggest that these variables are strongly coupled. To account for this interdependence, we can develop a scaling argument that will allow us to predict void content and demonstrate its dependence upon the physical interactions between phases. From thermal

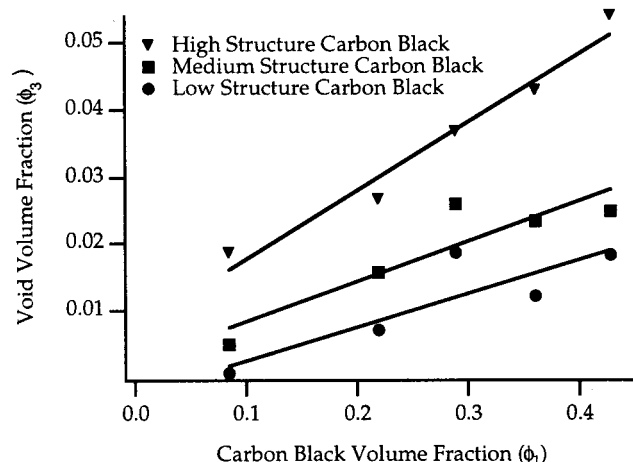


Figure 6. Annealed composite void content as a function of filler concentration for carbon blacks of various structure.

studies, we have seen that voids are absent in the melt, indicating carbon black is fully wet by the amorphous polymer, and appear concurrently with the onset of polymer crystallization. As we have verified the absence of significant void formation in pure room-temperature polyethylene samples, there must exist a strong interaction between polyethylene and the carbon black surface that is sufficient to induce the formation of voids upon crystallization. We therefore believe that the volume of voids incorporated will be a product of some measure of the amount of polymer/filler interaction and the extent of matrix crystallization. We assume here that the extent of interaction between the filler and polymer matrix will be proportional to the accessible filler surface area, which is dependent upon particle structure and concentration. Carbon black structure is often defined in terms of the dibutyl phthalate (DBP) adsorption value, a measure of the filler surface area per unit weight capable of being contacted or wet by DBP. By assuming similar mechanisms for polyethylene, we approximate the wettable filler surface area within the entire composite as being proportional to the product of the DBP value and mass of carbon black ($\rho_1 V_1$). The extent of matrix crystallization can be quantified as $\chi\phi_2$, where χ represents the fraction of crystallinity in the polymer phase, ϕ_2 . For lack of a specific mechanism, we will assume that the void content within a composite is simply proportional to both the volume fraction of crystalline polymer ($\chi\phi_2$) and our measure of carbon black/polyethylene interaction, the wettable filler surface area. Although not based upon detailed physics, this approach provides a means of treating samples of very different structure and composition within a uniform framework. This argument results in

$$V_3 \propto \text{DBP} \rho_1 V_1 \phi_2 \quad (1)$$

or, upon eliminating constants, as

$$\phi_3 \propto \text{DBP} \phi_1 \chi \phi_2 \equiv \psi \quad (2)$$

As suggested by this expression, polymer crystallinity, which is sensitive to variations in processing conditions, will strongly influence composite void content after crystallization. For composites of varying crystallinity, therefore, one must expect their void contents to differ by an amount proportional to the difference in their crystalline content. To investigate this issue, we have

Table 4. Composite Crystallinity Results

carbon black DBP value	vol fraction carbon black	quenched dPE % crystallinity $\pm 2\%$	annealed dPE % crystallinity $\pm 2\%$
112	0.36	73	81
112	0.29	73	78
80	0.429	73	75
80	0.36	73	74
80	0.29	72	80
80	0.22	73	80
56	0.29	75	78

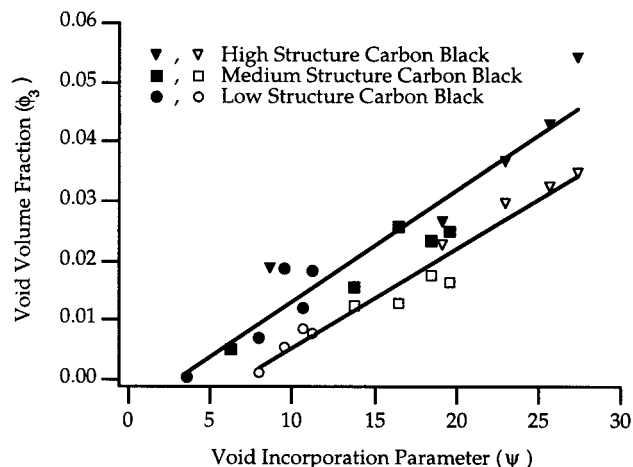


Figure 7. Void content plotted against the void incorporation parameter, ψ . Annealed (\blacktriangledown , \blacksquare , \bullet) and quenched (\triangledown , \square , \circ) composites are shown.

modified the crystalline content by performing postprocessing quenches from the melt. Crystallinity measurements as determined by WAXS are summarized in Table 4 and clearly show the effect of this thermal treatment on composite crystallinity relative to annealed samples. From eq 2, we expect quenched composites to incorporate voids to a lesser degree than annealed composites because quenching typically reduces the crystallinity by up to 10%. Void contents for quenched samples are displayed with those of the annealed samples versus ψ in Figure 7. From this figure, it is clear that the data for both thermal treatments collapse to lines, indicating the correct physical origins of void formation in these systems have been identified. The consistently lower void content for quenched relative to annealed composites also verifies the influence of crystallinity in both the formation and extent of the void phase. The data of Figure 7 do not collapse to a single curve, however, and instead form discrete lines which are representative of their respective thermal treatment. This behavior indicates that our assumption of a linear dependence of void content on matrix crystallinity does not fully capture the physical response within these systems as the dependence is stronger than we had assumed. Therefore, to arrive at a more sophisticated relationship that fully describes the physical mechanism of void incorporation, a better understanding of the detailed physics of the carbon black/polyethylene interface is required.

As discussed previously, our analysis allows calculation of void size in addition to content. Since no significant trend was observed in void size with volume fraction, Figure 8 shows void chord lengths averaged over all measured volume fractions as a function of filler structure for both annealed and quenched composites. These results clearly show an increase in the average size of void domains with increasing DBP values, yet

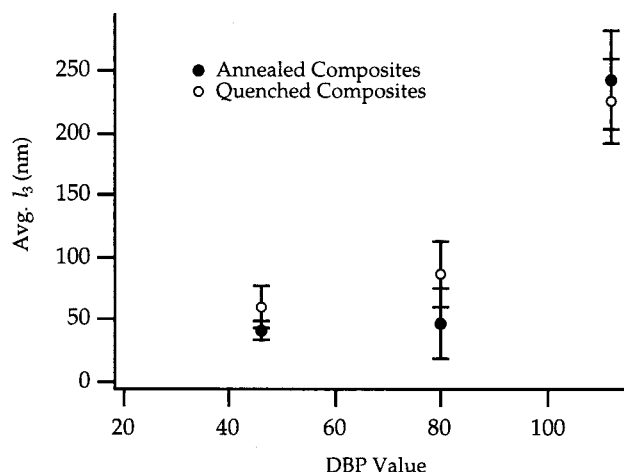


Figure 8. Chord lengths of the void phase (I_3) for composites containing carbon blacks of low (DBP = 46), medium (DBP = 80), and high (DBP = 112) structure averaged over all formulated filler volume fractions.

no evident effect as a result of varying crystallinity. This trend coupled with temperature excursion results and the strong correlation seen between void content and both filler structure and volume fraction suggest that carbon black structure alone dictates void size, while filler concentration, structure, and matrix crystallinity combine to directly influence overall void content. We have demonstrated that filler/polymer interactions can be studied by altering carbon black surface area and bulk polymer crystallinity. To fully elucidate the mechanism by which carbon black and polyethylene produce voids, however, we must better understand the specific interactions between filler surface and polymer matrix. Other studies have demonstrated that polymers strongly adsorb to the surface of carbon black particles during processing, resulting in an amorphous layer referred to as carbon gel or bound polymer.²⁰ It is quite possible that this strongly interacting polymer fraction plays a significant role in the void formation mechanism. Bound polymer can arise from chemical or physical interactions between the polymer and carbon black,²⁰ while filler surface area, structure, and surface activity, among other factors, dictate the amount formed.²¹ The process through which carbon black is manufactured defines the specific surface chemistry in addition to the structure and size of the particle. Therefore, changing the surface chemistry of carbon black particles may provide a means of tuning the adhesion of polymer to filler and thereby the amount of bound polymer and void formation within composite materials. It is also interesting to note that void content approaches zero at low values of ψ . If filler surface/bound polymer interactions do indeed dictate void development, then a critical filler volume fraction may exist below which the action of polymer crystallization in the bulk is unaffected by the presence of filler. Future work will focus on the effect of both surface chemistry modification and low filler volume fractions on void morphology to help complete our understanding of void formation and structure evolution during the processing of polyethylene/carbon black composite materials.

Conclusions

By using small-angle neutron scattering to identify the size and concentration of voids in carbon black/

polyethylene composites, several key parameters affecting void formation have been identified. In the melt, void content decreases to nearly zero and increases sharply with the onset of matrix crystallization. Void content also depends strongly upon both carbon black structure and concentration, which can be characterized by an overall wettable filler surface area. Combining the volume fraction of polymer present within the composite with this carbon black surface area, we have arrived at a scaling relationship that describes our data extremely well. Thermal treatments have also been used to influence the extent of crystallinity and elucidate the sensitivity of void incorporation to processing conditions. These results illustrate the critical role of both polymer recrystallization and filler structure in the void formation mechanism.

Acknowledgment. We thank Gordon Spellman at Lawrence Livermore National Laboratories for supplying deuterated polyethylene, Derek Leong at Raychem Corporation for TEM images, and Don Williamson of the Colorado School of Mines Physics Department for valuable assistance with SAXS experiments. We acknowledge the support of the National Institute of Standards and Technology, U.S. Department of Commerce, in providing the neutron research facilities used in this work. This material is based upon activities supported by the National Science Foundation under Agreement No. DMR-9423101.

References and Notes

- (1) Tang, H.; Chen, X.; Luo, Y. *Eur. Polym. J.* **1997**, *33*, 1383–1386.
- (2) Carmona, F. *Physica A* **1989**, *157*, 461–469.
- (3) Heaney, M. B. *Phys. Rev. B* **1995**, *52*, 12477–12480.
- (4) Viswanathan, R.; Heaney, M. B. *Phys. Rev. Lett.* **1995**, *75*, 4433–4436.
- (5) Doljack, F. A. *IEEE Trans. Comput., Hybrids, Manuf. Technol.* **1981**, *CHMT-4*, 372–378.
- (6) Oakes, J. A.; Sandberg, C. L. *IEEE Trans. Ind. Appl.* **1973**, *IA-9*, 462–466.
- (7) Wignall, G. D.; Farrar, N. R.; Morris, S. *J. Mater. Sci.* **1990**, *25*, 69–75.
- (8) Marr, D. W. M.; Wartenberg, M.; Schwartz, K. B.; Agamalian, M. M.; Wignall, G. D. *Macromolecules* **1997**, *30*, 2120–2124.
- (9) Wu, W.-L. *Polymer* **1982**, *23*, 1907–1912.
- (10) Debye, P.; Bueche, A. M. *J. Appl. Phys.* **1949**, *20*, 518–525.
- (11) Debye, P.; Anderson, H. R. J.; Brumberger, H. *J. Appl. Phys.* **1957**, *28*, 679–683.
- (12) Cheung, Y. W.; Stein, R. S.; Wignall, G. D.; Yang, H. E. *Macromolecules* **1993**, *26*, 5365–5371.
- (13) Marr, D. W. M. *Macromolecules* **1995**, *28*, 8470–8476.
- (14) DACA Instruments, Santa Barbara, CA.
- (15) Wignall, G. D.; Bates, F. S. *J. Appl. Crystallogr.* **1987**, *20*.
- (16) Dubner, W. S.; Schultz, J. M.; Wignall, G. D. *J. Appl. Crystallogr.* **1990**, *23*, 469–475.
- (17) Williamson, D. L.; Mahan, A. H.; Nelson, B. P.; Crandall, R. S. *Appl. Phys. Lett.* **1989**, *55*, 783–785.
- (18) Williamson, D. L. *Mater. Res. Soc. Symp. Proc.* **1995**, *377*, 251–262.
- (19) Schwartz, K. B.; Cheng, J.; Reddy, V. N.; Fone, M.; Fisher, H. P. *Adv. X-ray Anal.* **1995**, *38*, 495–502.
- (20) Kida, N.; Ito, M.; Kaido, H. *J. Appl. Polym. Sci.* **1996**, *61*, 1345–1350.
- (21) Leblanc, J. L.; Stragliati, B. *J. Appl. Polym. Sci.* **1997**, *63*, 959–970.
- (22) From manufacturer product literature; determined following ASTM Designation: D 3849-89.
- (23) From manufacturer product literature; determined following ASTM Designation: D 2414-91.

MA990160Z